SLAC-PUB-11860
May 2006

Elliptically Polarized Modes in RF Cavities *

G. Stupakov and K. Bane,
Stanford Linear Accelerator Center, Stanford University, Stanford, CA 94309 USA

Abstract

We study conditions under which a perturbation in boundary conditions of a cavity causes two modes with close frequencies to coalesce into elliptically polarized eigenmodes. We find that a surface impedance that is complex and varies with position along the cavity wall can give rise to elliptically polarized modes. For a simple two dimensional model our analytical perturbation results agree well with numerical simulations. We further demonstrate that a small variation in cavity shape can suppress mode ellipticity. Finally, we discuss the excitation of elliptical modes by bunch trains passing through the linac cavities in the ILC.

*Work supported by Department of Energy contract DE–AC02–76SF00515.

Elliptically Polarized Modes in RF Cavities

G. Stupakov and K. Bane

1 Introduction

Elliptically polarized eigenmodes have recently been found in computer simulation for the prototype RF structures for the linac of the International Linear Collider (ILC)[1]. These cavities have three couplers located at various azimuthal positions on the cavity wall in a way that breaks the azimuthal symmetry of the cavity. The modes are dipole modes, and the concern is that horizontal oscillation of a leading bunch in a bunch train can couple, through such modes, into the vertical plane and spoil the projected emittance of trailing bunches in the train. In this report, motivated by the numerical observation, we use perturbation theory to understand the basic physical mechanism leading to the existence of elliptically polarized modes. Then, for a concrete example, our theoretical results are applied to a simplified model of an RF cavity.

It is well known that the eigenmodes of the electromagnetic field in a cavity with perfectly conducting walls have linear polarization (see *e.g.* [2]). This means that the trajectory drawn by the end point of the vector of electric (or magnetic) field oscillating at a given location in the cavity (at the eigenfrequency of the mode) is a straight line. This is due to the fact that the equations for the eigenmodes have real coefficients when the boundary conditions are real. The solution to these equations can always be chosen as a real vectorial function, which corresponds to linear polarization[1].

The conductivity of metallic walls is normally finite but large, and its effect can be taken into account with the so called Leontovich boundary condition [2], which involves complex numbers. Strictly speaking, such a boundary condition gives rise to elliptically polarized eigenmodes; however, for non-degenerate modes the ellipticity is very small, on the order of the ratio of the skin depth to the reduced wavelength of the mode. On the same order is the ratio of the damping decrement of the mode to its frequency; hence the ellipticity is also on the order of the inverse quality factor Q of the mode.

The situation may be different if due to a symmetry in cavity shape there are degenerate modes. For example, in a cylindrically-symmetric cavity the transverse modes of different polarizations are always degenerate. In this case, in principle, a coupling introduced by the wall resistivity may result in a large elliptic polarization of the modes when resistivity is taken into account. As

[1] In the case of degenerate modes, the choice of eigenfunctions is not unique; however, they can always be chosen in such a way that each degenerate mode is linearly polarized.

we will show below, however, this can happen only when the wall resistivity is non-uniform over the wall. Although in practice a variation in wall conductivity is unlikely to be encountered, RF couplers can be thought of as sites of differing effective conductivity. We will accept this viewpoint in our analysis below.

We begin in Section 2 of this report by presenting a general analysis based on perturbation theory. We show how the boundary conditions affect mode coupling and under what conditions elliptic modes can be observed. In Section 3, this analysis is applied to the case of TM_{11} modes in a cylindrical cavity. In Section 4 a numerical result for the case of nonuniform boundary conditions is obtained and compared with the analytical theory. The effect of slight boundary distortion is also explored. Finally, in Section 5 we discuss implications of elliptically polarized modes on ILC performance. Note that throughout this report Gaussian units will be used.

2 Perturbation Theory and Eigenmodes

Let us consider an RF cavity and assume that the cavity's eigenmodes, in the approximation perfectly conducting walls, are known. For the s^{th} eigenmode we denote the frequency by ω_s, and the electric and magnetic fields by $\boldsymbol{E}_s$ and $\boldsymbol{H}_s$. We assume a time variation in the fields $\propto e^{-i\omega t}$.

To take into account metallic walls with finite conductivity, one can use the Leontovich boundary condition at the walls: [2]

$$\boldsymbol{E}_t = \zeta \boldsymbol{H}_t \times \boldsymbol{n}\,, \tag{1}$$

where $\boldsymbol{E}_t$ and $\boldsymbol{H}_t$ are the tangential components of the electric and magnetic fields and $\boldsymbol{n}$ is a unit vector directed into the metal; $\zeta = (1-i)\sqrt{\omega/8\pi\sigma}$, with σ the wall conductivity. This condition is valid if the skin depth corresponding to the frequency ω is much smaller than the wavelength of the mode.

In this paper, however, we will use the boundary condition Eq. (1) in a more general sense understanding the complex constant ζ as a phenomenological parameter responsible for possible losses in the wall. With such a parameter, for example, one can model coupling devices which connect the cavity to external waveguides. In this case ζ takes nonzero values only at the location of the coupler with the real part of ζ responsible for the energy loss transmitted through the coupler (hence $\mathrm{Re}\,\zeta > 0$) and the imaginary part due to the reactive component of the coupling.

We will use perturbation theory to calculate the effect of the generalized boundary condition (1) on the eigenmodes of the cavity. Our analysis is based on the method presented in Ref. [3] which will be outlined below. The perturbation theory is valid if the frequency change of the modes due to the boundary perturbation, $\Delta\omega_s$, is small: $|\Delta\omega_s/\omega_s| \ll 1$.

From the point of view of electromagnetic theory the boundary condition Eq. (1) can equivalently be represented as a surface magnetic current $\boldsymbol{\iota}$ flowing

in the vicinity of perfectly conducting walls

$$\boldsymbol{\iota} = -\frac{c}{4\pi}\zeta \boldsymbol{n} \times [\boldsymbol{n} \times \boldsymbol{H}]|_{\rm wall}\,. \tag{2}$$

This current has dimensions of magnetic charge per unit time per unit length.

Let us assume that the current $\boldsymbol{\iota}$ oscillates at frequency ω. It will excite an electromagnetic field $\boldsymbol{E}$ in the cavity that can be represented as a sum of eigenmodes (more precisely, the sum represents only the transverse part of the excited field, see [3]):

$$\boldsymbol{E} = \sum_s A_s \boldsymbol{E}_s\,, \tag{3}$$

where the coefficients A_s are given by

$$A_s = \frac{i\omega_s}{\omega^2 - \omega_s^2} b_s\,, \tag{4}$$

with

$$b_s = \frac{1}{N_s}\int \boldsymbol{\iota}\cdot\boldsymbol{H}_s\, dS\,, \tag{5}$$

and the mode norm N_s

$$N_s = \frac{1}{4\pi}\int \boldsymbol{E}_s^2\, dV\,. \tag{6}$$

The integration in Eq. (5) is performed over the boundary surface, that in Eq. (6) over the volume of the cavity.

Equations (3)-(6) can be used to find the frequency change from ω_s to ω due to the surface impedance ζ. First, we consider this calculation in the case of a nondegenerate mode which we denote by $s = 0$. In this case the dominant term in the sum in Eq. (3) will be $A_0\boldsymbol{E}_0$, with magnetic current $\boldsymbol{\iota} = A_0\boldsymbol{\iota}_0$, where

$$\boldsymbol{\iota}_0 = -\frac{c}{4\pi}\zeta \boldsymbol{n} \times [\boldsymbol{n} \times \boldsymbol{H}_0]|_{\rm wall}\,. \tag{7}$$

Rewriting Eq. (5) as

$$b_0 = \frac{A_0}{N_0}\int \boldsymbol{\iota}_0\cdot\boldsymbol{H}_0\, dS\,, \tag{8}$$

and substituting into Eq. (4) (with $s = 0$), we obtain an equation for frequency of the perturbed mode ω:

$$\omega^2 - \omega_0^2 = \frac{i\omega_0}{N_0}\int \boldsymbol{\iota}_0\cdot\boldsymbol{H}_0\, dS\,. \tag{9}$$

One can use this expression *e.g.* for calculating frequency shift of a mode due to wall resistivity or due to a small perturbation in cavity shape (the Slater formula) [3].

For the purposes of this paper, we need to generalize the above derivation to the case when there are two modes, 1 and 2, with close unperturbed frequencies ω_1 and ω_2 ($|\omega_1 - \omega_2| \ll \omega_1$). Let us assume that the dominant contribution to the

field comes from these two modes; we can write Eq. (3) as $\boldsymbol{E} = A_1\boldsymbol{E}_1 + A_2\boldsymbol{E}_2$. The magnetic current in the eigenmode is given by

$$\boldsymbol{\iota} = A_1\boldsymbol{\iota}_1 + A_2\boldsymbol{\iota}_2\,, \tag{10}$$

with

$$\boldsymbol{\iota}_s = -\frac{c}{4\pi}\zeta\boldsymbol{n}\times[\boldsymbol{n}\times\boldsymbol{H}_s]|_{\rm wall}\,, \qquad s=1,2\,. \tag{11}$$

Introducing the four coefficients

$$b_{sp} = \frac{1}{N_s}\int \boldsymbol{\iota}_p\cdot\boldsymbol{H}_s\,dS\,, \qquad s,p=1,2\,, \tag{12}$$

we write, corresponding to Eq. (4), the following two equations:

$$\frac{\omega^2-\omega_s^2}{i\omega_s}A_s = \sum_{p=1}^{2} b_{sp}A_p\,, \qquad s=1,2\,. \tag{13}$$

The two solutions ω of this system give the eigenfrequencies of the two perturbed modes, and the eigenvectors will be a linear combination of the original unperturbed modes. The equations can be used if the difference $|\omega_1-\omega_2| \ll |\omega|$; it is also applicable for the degenerate case when $\omega_1=\omega_2$.

In the next section we will apply these equation for the analysis of TM_{11} modes in a cylindrical cavity.

3 Cylindrical Cavity

We consider now a TM_{11} mode in a cylindrical cavity of radius a, with the z axis directed along the axis of the cylinder. To simplify the analysis we will assume that $k_z=0$, which means that the electromagnetic field has only the components E_z, H_r and H_θ which do not depend on z. This reduces our problem to two dimensions in the plane perpendicular to the z axis. The integration over the volume V in the equations of the previous section should be understood now as integration over the cylindrical cross-section and the integration over the surface S is now understood as integration over the boundary of this cross-section—the circle of radius a.

There are two TM_{11} degenerate modes with orthogonal polarizations in the cylindrical cavity with perfectly conducting walls. The E_z field in the modes is given by the following equation

$$E_z = J_1\left(\frac{\nu_{11}r}{a}\right)\begin{Bmatrix}\cos\theta\\ \sin\theta\end{Bmatrix}\,, \tag{14}$$

where ν_{11} is the first root of the Bessel function J_1 (we choose our overall coefficient to be 1). The frequency of these modes is $\omega_1=\omega_2=c\nu_{11}/a$. The azimuthal component of magnetic field in the modes is given by

$$H_\theta = \frac{ic}{\omega}\frac{\partial E_z}{\partial r} = \frac{ic\nu_{11}}{\omega a}J_1'\left(\frac{\nu_{11}r}{a}\right)\begin{Bmatrix}\cos\theta\\ \sin\theta\end{Bmatrix} = iJ_1'\left(\frac{\nu_{11}r}{a}\right)\begin{Bmatrix}\cos\theta\\ \sin\theta\end{Bmatrix}\,, \tag{15}$$

where the prime denotes the derivative with respect to the argument. The norm of the modes given by Eq. (6) is

$$N_{1,2} = \frac{1}{4\pi}\int E_z^2 r\, dr d\theta = \frac{1}{4}\int_0^a J_1^2\left(\frac{\nu_{11} r}{a}\right) r\, dr = -\frac{a^2}{8} J_0(\nu_{11}) J_2(\nu_{11})\,. \quad (16)$$

The two modes are linearly polarized. This means that the vector of the magnetic field at a given location oscillates in time in such a way that its end point moves along a straight line (the polarization line). The polarization lines for the two modes are perpendicular to each other.

Let us now assume that there is a surface impedance which depends on the position on the wall $\zeta(\theta)$. Using the theory of the previous section we will calculate the perturbed eigenmodes and eigenfrequencies of the two degenerate modes described above.

The magnetic current of the surface, given by Eq. (11), now has only a θ component:

$$\iota_\theta = \frac{c}{4\pi}\zeta(\theta) H_\theta\,. \quad (17)$$

Using Eqs. (15), (16) and (17) we can calculate the coefficients b_{sp} in Eq. (12):

$$b_{sp} = \frac{2c J_1'^2(\nu_1)}{\pi a J_0(\nu_1) J_2(\nu_1)} h_{sp}\,, \quad (18)$$

where

$$\begin{aligned} h_{11} &= \int_0^{2\pi} d\theta \zeta(\theta)\cos^2\theta\,, \\ h_{12} = h_{21} &= \int_0^{2\pi} d\theta \zeta(\theta)\cos\theta\sin\theta\,, \\ h_{22} &= \int_0^{2\pi} d\theta \zeta(\theta)\sin^2\theta\,. \end{aligned} \quad (19)$$

Introducing $\Delta\omega = \omega - \omega_s$ and using $\omega^2 - \omega_s^2 \approx 2\omega_s\Delta\omega$ we can write Eq. (13) in the following dimensionless form

$$\Lambda A_s = \sum_{p=1}^{2} h_{sp} A_p\,, \quad (20)$$

where

$$\Lambda = \frac{\Delta\omega}{\omega}\frac{\pi\nu_1 J_0(\nu_1) J_2(\nu_1)}{i J_1'^2(\nu_1)}\,. \quad (21)$$

Solving the system of equations (20) and finding two eigenvalues $\Lambda_{1,2}$ gives the frequency shifts $\Delta\omega_{1,2}$ of the two modes. The corresponding eigenvectors $\{A_1, A_2\}$ define the coupling of the original linearly polarized modes in the new perturbed eigenmodes. Note, that elliptic polarization of the modes occurs only if the ratio A_1/A_2 is a complex number.

If ζ does not depend on θ, then it can be eliminated from the system by the transformation $\Lambda \to \Lambda\zeta$. The resulting system of linear equations is symmetric with real coefficients, and has real eigenvectors corresponding to linearly polarized perturbed eigenmodes. Hence even a complex surface conductivity does not guarantee elliptical polarization of modes, unless the conductivity is non-uniform along the surface.

As a specific example, consider now the case where two short strips of the wall, of angular length $\Delta\theta \ll \pi$, have surface conductivities ζ_1 and ζ_2, respectively (see Fig. 1). The angular distance between the segments is equal to α.

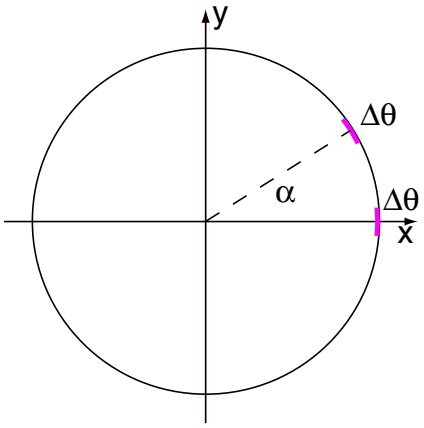

Figure 1: The geometry of the 2D round cavity with two conducting short segments shown in color.

The matrix elements are now approximately equal to

$$\begin{aligned} h_{11} &= \Delta\theta(\zeta_1 + \zeta_2 \cos^2\alpha)\,, \\ h_{12} = h_{21} &= \Delta\theta\zeta_2 \cos\alpha \sin\alpha\,, \\ h_{22} &= \Delta\theta\zeta_2 \sin^2\alpha\,. \end{aligned} \tag{22}$$

Eq. (20) can be solved analytically, yielding eigenvalues

$$\Lambda_{1,2} = \frac{\Delta\theta}{2}\left(\zeta_1 + \zeta_2 \pm \sqrt{\zeta_1^2 + 2\zeta_2\zeta_1\cos 2\alpha + \zeta_2^2}\right)\,, \tag{23}$$

with corresponding eigenvectors

$$\{A_1, A_2\} = \left\{-\frac{1}{\zeta_2 \sin 2\alpha}\left(\zeta_1 + \zeta_2\cos 2\alpha \mp \sqrt{\zeta_1^2 + 2\zeta_2\zeta_1\cos 2\alpha + \zeta_2^2}\right), 1\right\}\,. \tag{24}$$

A complex value of the eigenvector means that the resulting eigenmode is elliptically polarized—the end point of the magnetic field moves with time along

an ellipse. The two important parameters of this polarization ellipse are the axes ratio R (≤ 1) and the tilt angle ψ relative to the x axis. They can be expressed in terms of the absolute value $|A|$ and the argument δ of the ratio $A = A_1/A_2$, $A = |A|e^{i\delta}$:

$$R = \left| \frac{S_+ - S_-}{S_+ + S_-} \right| , \qquad \tan 2\psi = \frac{2|A| \cos\delta}{|A|^2 - 1} , \tag{25}$$

where $S_\pm = \sqrt{|A|^2 + 1 \pm 2|A| \sin\delta}$.

To illustrate how the polarization ellipse parameter R depends on parameters ζ_1, ζ_2, and the angle α we carried out calculations for the case when the surface impedances of the two segments have the same absolute value and differ only in phase: $\zeta_1 = e^{i\phi}\zeta_2$, where ϕ is a real parameter. Fig. 2 shows the dependence of R on the angle α for several values of ϕ. It is seen from this figure that depending

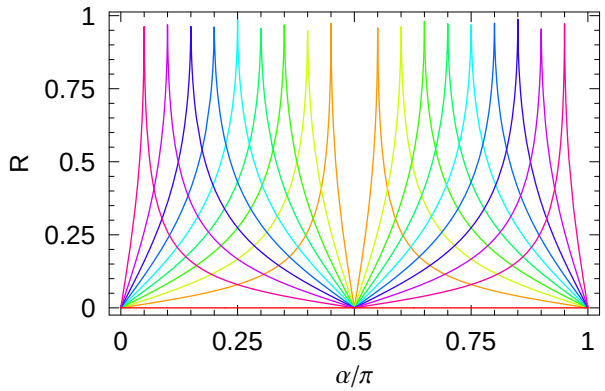

Figure 2: The dependence of the axes ratio R versus the angle α for several values of ϕ, from $\phi = 0.1$ to $\phi = 0.9$ with the step 0.1 (curves with smaller values of ϕ have peaks closer to the center).

on the ratio of the surface conductivities, one can always find a position for the segments which gives the maximum ellipticity factor R. The peaks for maximal R are rather narrow, however. Note also that for the case $\alpha = 90^\circ$ the ellipticity is always zero (linear polarization).

4 Simulations

For numerical simulations we used the Matlab toolbox, Pdetool. It is a 2D finite element, partial differential equation solver. We use it to solve the Helmholtz equation for E_z:

$$\nabla^2 E_z + \lambda E_z = 0 \tag{26}$$

with boundary conditions. The solutions of Eq. 26 are eigenfunctions E_{zn} with eigenvalues $\lambda_n = \omega_n^2/c^2$. For our model calculations the beam pipe has radius $a = 0.5$ (dimensionless). For boundary condition we take $E_z = 0$ everywhere except for two strips of length $\Delta\theta = 18°$, whose centers are located at angles $\theta = 0°$ and $\theta = \alpha = 44°$ with respect to the x-axis (see Fig. 1). For the upper/lower strip we choose parameter $\zeta = 0.0185(0.88 \pm i)$. Both boundary conditions indicate loss, though one strip is inductive, the other capacitive. The parameters α and ζ were chosen to give modes with substantial ellipticity. For the calculation 50,000 mesh points were used (part of the mesh is shown in Fig. 3). Note that our numerical method does not assume that ζ (or $\Delta\theta$) is small, and hence goes beyond the range of applicability of the perturbation theory.

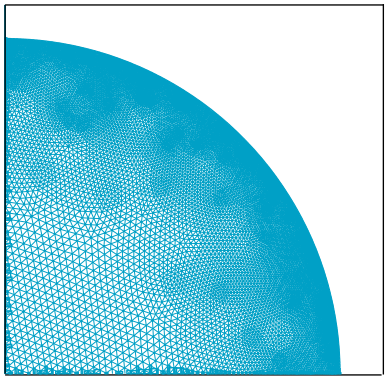

Figure 3: Mesh used in one quarter of the domain of calculation.

The numerical calculation yields two lowest dipole modes with eigenvalues:[2] $\lambda_1 = 58.745(1.00001 - 0.00027i)$ and $\lambda_2 = 58.745(1.00020 - 0.00029i)$; the equivalent Q's of the modes ($Q = \mathrm{Re}\,(\lambda)/\mathrm{Im}\,(\lambda)$) are $Q_1 = 3700$ and $Q_2 = 3400$. In Fig. 4 density plots of the numerically obtained $\mathrm{Im}\,(E_z)$ (left) and $\mathrm{Re}\,(E_z)$ (right) for one of the modes are given. Violet indicates positive and blue negative field values. Note that according to the Panofsky-Wenzel theorem the transverse wake force is just proportional to the gradient of the field plotted here.

In the case of linearly polarized modes the real and imaginary parts of the solution would be oriented in the same or opposing direction. From Fig. 4 we see that this is not the case; and since the two parts of E_z are comparable in amplitude, we expect this mode to have significant polarization ellipse parameter R. We fit both parts of E_z to

$$AJ_1\left(\frac{\nu_{11}r}{a}\right)\cos(\theta - \delta)$$

[2]Note that the mode frequencies are shifted up slightly from the ideal, perfectly conducting case, where $\lambda = (\nu_{11}/a)^2 = 58.728$. This is primarily an artifact of the boundary actually used in the simulation—a 180 sided inscribed, equilateral polygon, rather than a circle.

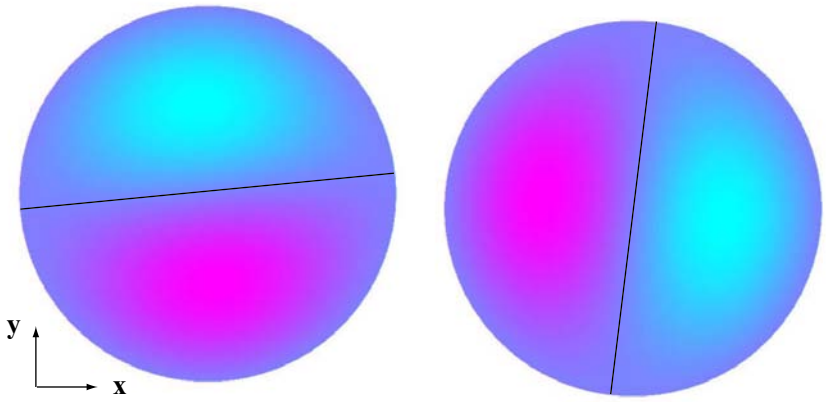

Figure 4: Numerically obtained density plots of $\mathrm{Im}\,(E_z)$ (left) and $\mathrm{Re}\,(E_z)$ (right) for a first dipole mode for our model problem (round pipe case). Violet (blue) indicates positive (negative) field values. The node lines of the analytical fits (at angles $\theta = \delta + \pi/2$) are also shown.

for amplitude A and orientation angle δ. The fits are good, with a maximum deviation $< 1\%$. [Note that in Fig. 4 the node lines of the analytical fits (at angle $\theta = \delta + \pi/2$) are also displayed.] Then using Eqs. 25, we obtain the polarization ellipse parameters $R = 0.64$ and tilt angle $\psi = -16°$. Note that the second eigenmode has the same R though with the tilt angle rotated by $\pi/2$.

If we reduce the strip length by a factor of 3 to $\Delta\theta = 6°$ and scale the boundary condition up by a factor of 3 we might expect to obtain similar results. In fact, however, the numerically obtained Q's of the two modes are no longer approximately equal ($Q_1 = 5500$, $Q_1 = 2600$); in addition, $R = 0.52$ and $\psi = -42°$. These results are not in agreement with our analytical perturbation calculation. We find that, for short boundary strips, the step-like change in boundary condition at the edge of the strips invalidates the applicability of the perturbation calculation. This is due to the fact that the magnetic field $\boldsymbol{H}$ in the vicinity of the strips differs from the value in the unperturbed mode even though $|\zeta| \ll 1$. A modified perturbation theory can be developed which takes this effect into account and is based on the smallness of the parameter $\Delta\theta \ll 1$ only. Such a theory, however, is beyond the scope of this paper. For longer strips the edge conditions become less important, and our perturbation method still holds.

4.1 Elliptically Distorted Boundary

In reality structures are never perfectly round, and we can imagine that a small change in the boundary shape can have a big effect on the rotating mode properties. Let us consider a slightly elliptical boundary. Slater's perturbation formula

for frequency change due to a small boundary change is given (in 2D) by

$$\frac{\delta\lambda}{\lambda} = \frac{\int_{\Delta\mathcal{A}}(E^2 - B^2)\,da}{\int_{\mathcal{A}} E^2\,da}\ , \tag{27}$$

with the numerator an integration over the area changed by the modification $\Delta\mathcal{A}$, and the denominator an integration over the entire cavity area $\mathcal{A}$. Let us consider a round structure of radius a distorted to an upright ellipse with x and y axes $a(1+\epsilon)$ and a, with ϵ a small parameter. According to Slater's formula, for this case, the frequency splitting of two TM_{11} modes becomes $\Delta\lambda/\lambda = \epsilon$. For a slightly elliptical structure, with perfect boundary conditions, the Pdetool program yields a frequency shift that is in good agreement with this result; for example, for $\epsilon = 10^{-3}$ the program yields $\Delta\lambda/\lambda = 1.004 \times 10^{-3}$.

The equations of the perturbation theory for the case of elliptically distorted boundaries become

$$\Lambda_s A_s = \sum_{p=1}^{2} h_{sp} A_p\,, \tag{28}$$

where

$$\Lambda_s = \frac{\Delta\omega - \delta\omega_s^{(e)}}{\omega}\,\frac{\pi\nu_1 J_0(\nu_1)J_2(\nu_1)}{iJ_1'^{\,2}(\nu_1)}\,, \tag{29}$$

with $\delta\omega_s^{(e)} = (\delta\lambda/\lambda)\omega$ being the frequency change of the mode due to ellipticity of the cross section. The coefficients h_{sp} in this equation can still be calculated from Eqs. (19) due to the assumed smallness of the boundary distortion.

In Table 1 we present numerical results for our model problem, but now with slightly distorted elliptical boundaries, for several values of ϵ. Given are the relative frequency splitting $\mathrm{Re}\,(\Delta\lambda/\lambda)$ and the Q's of the modes; the polarization ellipse parameters R and the tilt angle ψ for one mode (for the other mode, R is the same but ψ is rotated by $\pi/2$). We see that frequency splitting is minimized and R is maximized in the round case ($\epsilon = 0$). Also, as expected, R is significant only for $\epsilon \lesssim 1/Q$. We also see that for elliptical boundaries, the Q's of the two modes can become quite dissimilar.

In Fig. 5 we plot R from the table (the plotting symbols). Superimposed is the analytical perturbation solution, Eqs. (28) and (29). We see remarkably good agreement.

5 Discussion

The ILC RF structure, for which elliptically polarized modes were numerically found, has three couplers that break the cylindrical symmetry of the cavity: one fundamental mode coupler (downstream, at azimuthal angle $\theta = 0$) and two identical higher mode couplers (one upstream at $\theta = -30^\circ$ and one downstream at $\theta = -145^\circ$). Assuming our 2D analysis qualitatively holds also for this 3D geometry, we can say that our basic requirement for elliptically polarized

Table 1: Numerical results for our model problem with an elliptically distorted boundary. Parameters are $\alpha = 44°$, $\Delta\theta = 18°$, $\zeta = 0.0185(0.88 \pm i)$. The boundary ellipse is upright with x and y axes $a(1+\epsilon)$ and a. Given are the relative frequency split $\mathrm{Re}\,(\Delta\lambda/\lambda)$, the Q's of the modes; the ellipticity R and the tilt angle ψ for one mode (for the other mode R is the same, but with ψ rotated by $\pi/2$).

ϵ $[10^{-3}]$	$\mathrm{Re}\,(\Delta\lambda/\lambda)$ $[10^{-3}]$	Q_1 $[10^3]$	Q_2 $[10^3]$	R	$-\psi_1$ [deg]
-2.0	1.6	5.8	2.5	0.10	86
-1.0	0.6	7.6	2.3	0.19	76
-0.5	0.2	12.1	2.1	0.02	59
0.0	0.2	3.7	3.4	0.64	16
0.5	0.8	3.0	4.3	0.22	5
1.0	1.4	2.9	4.5	0.14	3
2.0	2.4	2.8	4.8	0.08	2

modes is satisfied: the "impedance" varies in a complex way with θ (the fundamental mode and higher mode couplers are completely different objects). Note, however, that the ILC structure is a 3D object, and the conditions for finding elliptically polarized modes are likely more varied in a 3D structure than for our 2D model. For example, for two identical boundary strips in the 2D problem, we can already see from the mirror symmetry of the structure that rotating modes do not exist; in the equivalent 3D case, however, if one boundary strip is upstream and the other downstream we no longer have such symmetry, and elliptically polarized modes are not *a priori* precluded.

If a bunch excites an elliptically polarized mode one needs to wait some time before a test particle will experience an elliptically polarized kick. The reason is that there are two elliptically polarized eigenmodes with nearly the same frequencies. The field excited by the bunch will be a superposition of the elliptic modes that is initially linearly polarized. After time $t \sim \pi/(2\Delta\omega)$, however, the relative phase of the modes starts to deviate significantly from its initial value, and the total field becomes elliptically polarized. For example, considering the nominal (round, $\epsilon = 0$) case in Table 1, we see that only after $\omega t \approx 2500$ behind the exciting bunch will this happen. For the ILC example, where the bunch spacing is 308 ns, and the dipole mode frequency is 1.8 GHz, if the mode is excited by the first bunch in a train this point is reached at 220 ns. Since $Q \approx 3500$, the damping time is 620 ns. Thus the wakefield reaches to only ~ 4 bunches behind the exciting bunch. In simulations for the real ILC 9-cell structure design many dipole modes are found with Q's typically $\sim 10^4$ [1]; for those that are elliptically polarized, the effect will move further back in the bunch train than calculated here.

We saw that if the cavity is out-of-round by more than an equivalent $\epsilon \sim 0.5 \times 10^{-3}$, then elliptical polarization is suppressed. If the Q of a mode is 10 times larger, as the simulations suggest, an out-of-roundness $\sim 10^{-4}$ is already enough

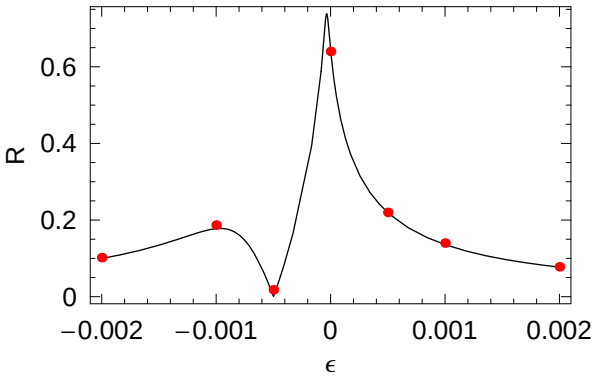

Figure 5: Polarization ellipse amplitude ratio R *vs* boundary ellipse parameter ϵ.

to preclude elliptical modes. Thus, in the real ILC cavities with manufacturing errors it is very possible that elliptical modes are precluded.

Finally we should mention that, from our point of view, elliptically polarized modes are quite interesting in themselves as a physical phenomenon. As a practical problem for the ILC, however, linearly polarized modes (with the polarization plane tilted relative to the x and y axes), which occur whenever there is broken symmetry in the cavity are just as dangerous for coupling x beam motion into the y plane.

6 Conclusion

In this paper we have studied conditions under which a perturbation in boundary conditions causes two modes with close frequencies to coalesce into elliptically polarized eigenmodes. We have found that a surface impedance that has a complex value and varies along the cavity wall leads to such elliptically polarized modes. For a simple two dimensional model our numerical simulations agree well with the analytical results of perturbation theory in its region of validity. We have also demonstrated that even a small variation in the cavity shape can suppress the ellipticity of such modes. And finally, we have discussed the excitation of elliptical modes by bunch trains passing though the linac cavities in the ILC.

Acknowledgements

The authors thank Kwok Ko and his group for explaining to us the results of their 3D numerical simulations. One of us (K.B.) thanks Zenghai Li for helpful discussions about elliptically polarized modes.

References

[1] K. Ko *et al*, "Advances in electromagnetic modelling through high performance computing", to be published in Physica C, 2006.

[2] L. D. Landau and E. M. Lifshitz, *Electrodynamics of Continuous Media*, Vol. 8 of *Course of Theoretical Physics* (Pergamon, London, 1960), 2nd ed., (Translated from the Russian).

[3] L. A. Vainshtein, *Electromagnetic Waves* (Radio i svyaz', Moscow, 1988), in Russian.